Enhanced diffusion in soft-walled channels with a periodically varying curvature

Thomas H. Gray [1], Claudio Castelnovo [1], and Ee Hou Yong [2,*]

[1] T.C.M. Group, Cavendish Laboratory, JJ Thomson Avenue, Cambridge CB3 0HE, United Kingdom

[2] Division of Physics and Applied Physics, School of Physical and Mathematical Sciences, Nanyang Technological University, Singapore 637371

(Received 12 July 2021; revised 30 March 2022; accepted 26 April 2022; published 24 May 2022)

The motion of particles along channels of finite width is known to be hindered by either the presence of energy barriers along the channel direction or by variations in the width of the channel in the transverse direction (rugged channel). Remarkably, when both features are present, they can interact to produce a counterintuitive result: adding energy barriers to a rugged channel can enhance the rate of diffusion along it. This is the result of competing energetic and entropic effects. Under the approximation of particles instantaneously in equilibrium in the transverse direction, one can tailor the energy barriers to the ruggedness to recover free diffusion. However, such fine-tuning and potentially restrictive approximations are not necessary to observe an enhanced rate of diffusion as we demonstrate by adding a range of (non-fine-tuned) energy barriers to a channel of sinusoidally varying curvature. Furthermore, this was observed to hold for systems with a finite characteristic timescale for motion in the transverse direction, thus, suggesting that the phenomenon lends itself to be exploited for practical applications.

DOI: 10.1103/PhysRevE.105.054141

I. INTRODUCTION

Transport processes in channels of varying profile have been studied for many years. With applications in disparate fields, such as zeolites and porous solids [1–3], biological membranes [4–6], separating particles by their size [7–9] and carbon nanotubes [10], the importance of understanding these systems' behaviors is clear.

The free diffusion of particles along a channel can be hindered by the introduction of either a series of energy barriers or variations in the width of the channel (ruggedness). Interestingly, combining the two features—adding barriers to a rugged channel or ruggedness to a channel with barriers—can sometimes increase the rate of diffusion along the channel. This counterintuitive phenomenon can be understood in a precise way in the limit where motion along the length of the channel is much slower than in the transverse direction so that the ensemble of particles can be assumed to be in instantaneous transverse equilibrium as it propagates. In this case, as we will review below, the motion is effectively a one-dimensional diffusion problem where the effect of the ruggedness enters through a modification to the one-dimensional potential along the line of the channel. It is then clear that one can trade ruggedness against energetic barriers to flatten the free-energy profile, and, in some instances, even restore free diffusion. This typically requires fine-tuning.

Here we investigate the case of overdamped motion in a soft-walled channel whose profile varies periodically. By introducing a (matching) periodic potential along the channel—for example, through the application of an external field (e.g., an electric field for charged particles in the channel [11])—we show that it is possible to increase the rate of diffusion above that observed without the potential for a range of phase shifts between the roughness and the barriers and for finite damping rates in the transverse direction. Our results demonstrate that the counterintuitive enhancement of diffusion along a rough channel upon the addition of energy barriers occurs also in realistic settings of potential practical interest.

The paper is structured as follows. Section II briefly reviews the relevant background knowledge and literature. Section III introduces the model and the main analytical results, which are then contrasted with numerical simulations that account for the finite relaxation time in the transverse direction in Sec. IV. The case of a channel with hard walls is considered for completeness in Sec. V. And we finally draw our conclusions in Sec. VI.

II. BACKGROUND

A common starting point in studying the motion of particles in finite-dimensional channels is the Fick-Jacobs equation, an effective one-dimensional equation for the evolution of the concentration of a solute along the center line of a multidimensional tube. Jacobs' treatment [12], which he attributed to Fick [13], was refined by Zwanzig [14], who produced a more general version. By assuming that the system is fully equilibrated in the confining direction, Zwanzig reduced the multidimensional Smoluchowski equation to a one-dimensional form with a modified potential. The changing profile of the channel produces a logarithmic contribution to this potential, which leads to the description of the effect upon the motion in terms of "entropic" barriers [15].

However, it is not always safe to assume that the system equilibrates fully in the confining direction; a profile which

*eehou@ntu.edu.sg

varies too rapidly, for instance, can prevent equilibrium from being established [16]. Zwanzig [14] acknowledged the limitations of this approach and suggested how small deviations from equilibrium might be accounted for. This work, based around a spatially varying diffusion coefficient, has been examined in various contexts and built upon heavily [17–21].

Adding potential energy barriers to a channel of varying width can cause interesting effects because of the interaction between the energetic and the entropic contributions to the potential. For instance, in the presence of a linear bias along the channel, tuning the phase difference between the periodic channel width and the periodic barriers can induce a resonancelike behavior in the nonlinear mobility, and rectification can be observed [22]. Another example involves a channel with cosine-shaped walls which connects two reservoirs of particles at different concentrations over one period. By introducing a cosine energy barrier along the channel, tuning the phase relative to the walls, and applying an oscillating and unbiased force along the channel, it is possible to produce transport from low to high concentration [23].

We note in passing that, although channels which are symmetrical about their center line feature prominently in this field, the more general case of a curved midline and varying width has also attracted attention. The motion can still be mapped onto one dimension, albeit with a modified expression for the spatially varying diffusion coefficient, which now reflects the variation in the midline of the channel [24–27]. Motion in serpentine channels where the midline is curved but the width is constant has also been studied [28,29]. Channels of curved midline and varying width can be created by using the same function to describe both walls but then introducing an offset between the two. The current can be affected by this shift, and a preferential direction of transport can emerge [30,31].

III. A ONE-DIMENSIONAL MODEL FOR THE EFFECTIVE DIFFUSION COEFFICIENT

We consider motion in a two-dimensional channel with soft walls in the transverse (y) direction,

$$U(x, y) = U_x(x) + U_y(x, y), \tag{1}$$

where U_x is the potential energy contribution along the channel and U_y describes how the profile of the channel varies as a function of the displacement along it. If the channel is periodic in x, then the long-time motion will be diffusive and can be described by an effective diffusion coefficient D_{eff}. We will use Zwanzig's derivation of the Fick-Jacobs equation to explore the system's behavior.

Zwanzig restricted his attention to the effect upon the diffusion coefficient of changes in the profile of the channel [14]. Here we will retain the effect of energy barriers. Our starting point is the two-dimensional Smoluchowski equation for the probability density $p(x, y, t)$,

$$\frac{\partial p}{\partial t} = D_x \frac{\partial}{\partial x} e^{-\beta U(x,y)} \frac{\partial}{\partial x} e^{\beta U(x,y)} p + D_y \frac{\partial}{\partial y} e^{-\beta U(x,y)} \frac{\partial}{\partial y} e^{\beta U(x,y)} p, \tag{2}$$

where D_x and D_y are the free diffusion coefficients in the x and y directions, respectively. By inserting Eq. (1) into Eq. (2), integrating over the y direction, and using the fact that U_y is confining, we obtain

$$\frac{\partial \rho}{\partial t} = D_x \frac{\partial}{\partial x} e^{-\beta U_x} \int_{-\infty}^{\infty} dy \left[e^{-\beta U_y} \frac{\partial}{\partial x} e^{\beta U_x + \beta U_y} p \right], \tag{3}$$

where $\rho(x, t) = \int_{-\infty}^{\infty} dy\, p(x, y, t)$ is the one-dimensional probability density. Let us assume that the distribution is always in equilibrium in the y direction, i.e.,

$$p(x, y, t) \approx \rho(x, t) \frac{e^{-\beta U_y(x,y)}}{e^{-\beta A(x)}}, \tag{4}$$

where $A(x)$ is defined through

$$e^{-\beta A(x)} = \int_{-\infty}^{\infty} dy\, e^{-\beta U_y(x,y)}. \tag{5}$$

This assumption is readily satisfied for systems with a high degree of diffusion anisotropy ($D_y \gg D_x$) or for systems where the profile of the channel $\alpha(x)$ varies sufficiently slowly along its length (x) for the ensemble of particles to remain in equilibrium in the confining direction (y), while spreading out along the length of the channel. To see this, consider the following argument. Suppose that the mean first-passage time to move one repeat unit (length L) in the x direction is τ_x, and the equilibration time in the y direction is τ_y. From the standard expression for the mean first-passage time, the former is proportional to L^2/D_x [32]. The mean-squared displacement of an ensemble of particles in a confining parabolic potential approaches equilibrium according to $1 - e^{-t/\tau}$, where $\tau \propto 1/D_y$. Although the potential is of infinite extent, equilibrium is attained after only a few multiples of τ have elapsed. Equilibrium in the confining direction can then be sustained throughout the motion provided that $\tau_y \ll \tau_x$ or, equivalently, $\tau_y/\tau_x \ll 1$. This condition leads to $D_x/L^2 D_y \ll 1$, which is satisfied for the two cases outlined above: highly anisotropic diffusion or a slowly varying channel profile (large L). Inserting Eq. (4) into Eq. (3) and carrying out the integration over y produces the following partial differential equation for the one-dimensional density,

$$\frac{\partial \rho}{\partial t} = D_x \frac{\partial}{\partial x} e^{-\beta U_x - \beta A} \frac{\partial}{\partial x} e^{\beta U_x + \beta A} \rho, \tag{6}$$

from which we can deduce the following expression for the one-dimensional effective potential U^* defined as

$$U^*(x) = U_x(x) - \frac{1}{\beta} \ln\left(\int_{-\infty}^{\infty} dy\, e^{-\beta U_y(x,y)} \right). \tag{7}$$

Before we restrict our attention to a particular channel it is worth remarking upon an implication of Eq. (7). Variations in the profile of the channel impede motion, a feature accounted for by the second term in the expression for the effective potential. However, Eq. (7) implies that this retarding effect can be countered by introducing a potential in the x direction: by setting $U_x = \frac{1}{\beta} \ln \int_{-\infty}^{\infty} dy\, e^{-\beta U_y(x,y)}$, the effective potential is zero, and free diffusion is predicted. This is a point to which we will return.

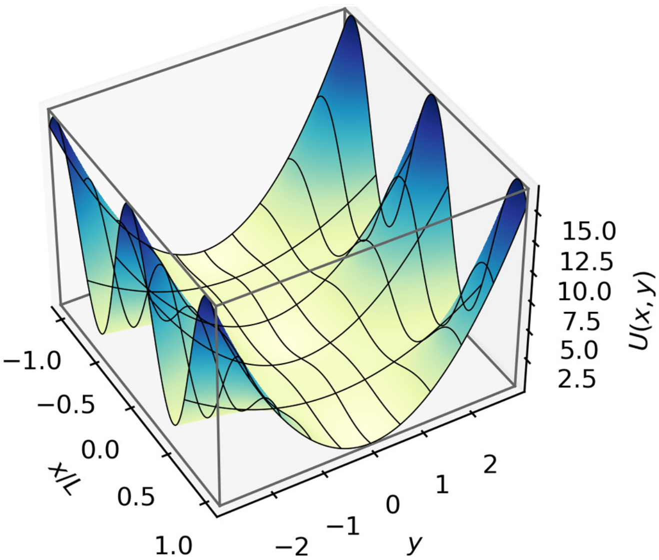

FIG. 1. A three-dimensional sketch of a section of the channel $U(x, y)$ described by Eq. (8) is shown for the following parameter values $\alpha_0 = 2$, $\alpha_1 = 1.8$, and $\beta Q = 1.255\,25$.

We now focus on the potential energy landscape,

$$U_x(x) = \frac{Q}{2}\left[1 + \cos\left(\frac{2\pi}{L}(x - \Delta x)\right)\right],$$
$$U_y(x, y) = \frac{1}{2}\left[\alpha_0 + \alpha_1 \cos\left(\frac{2\pi x}{L}\right)\right]y^2, \tag{8}$$

where $Q \geqslant 0$, and $\alpha_0 > \alpha_1$ to make the channel confining, and we study the effects of Q and Δx on the motion (see Fig. 1).

With the expression for the one-dimensional effective potential in Eq. (7), we can derive the effective diffusion coefficient by considering the mean first-passage time from the potential energy maximum at $x = \Delta x$ to either of the maxima at $x = \Delta x \pm NL$. This is given by

$$\tau_N = \frac{\mathcal{P}_R}{D_x}\int_{\Delta x}^{\Delta x+NL} dy\, e^{\beta U^*(y)} \int_{\Delta x - NL}^{y} dz\, e^{-\beta U^*(z)} - \frac{\mathcal{P}_L}{D_x}\int_{\Delta x-NL}^{\Delta x} dy\, e^{\beta U^*(y)} \int_{\Delta x - NL}^{y} dz\, e^{-\beta U^* z)}, \tag{9}$$

where $\mathcal{P}_L$ and $\mathcal{P}_R$ are the probabilities that the particle exits the region $[\Delta x - NL, \Delta x + NL]$ to the left and right, respectively [32]. The symmetry of the energy landscape means that $\mathcal{P}_L = \mathcal{P}_R = 1/2$, and Eq. (9) simplifies to

$$\tau_N = \frac{N^2}{2D_x}\int_{\Delta x}^{\Delta x+L} dy\, e^{\beta U^*(y)} \int_{\Delta x - L}^{\Delta x} dz\, e^{-\beta U^*(z)}, \tag{10}$$

where we have used the periodicity of the potential to recast each integral over one period.

After evaluating Eq. (7) for the specific potential defined in Eq. (8), inserting the result into Eq. (10), and changing variables to $\theta = 2\pi x/L$, we find

$$\tau_N = \frac{(NL)^2}{8\pi^2 D_x}\mathcal{I}_-\mathcal{I}_+, \tag{11}$$

where the quantities $\mathcal{I}_\pm$ are given by

$$\mathcal{I}_\pm = \int_{\phi}^{2\pi+\phi} d\theta\, \exp\left[\pm\frac{\beta Q}{2}\cos(\theta - \phi)\right][\alpha_0 + \alpha_1 \cos\theta]^{\pm 1/2}, \tag{12}$$

and $\phi = 2\pi\Delta x/L$ is the phase difference. Finally, we obtain the effective diffusion coefficient,

$$D_{\text{eff}} = \lim_{N\to\infty}\frac{(NL)^2}{2\tau_N} = \frac{4\pi^2 D_x}{\mathcal{I}_-\mathcal{I}_+}. \tag{13}$$

For some phases ϕ, the diffusion coefficient increases with increasing barrier height

The derivative of D_{eff} with respect to βQ can be an informative quantity because it describes the response of the system to an increase in the height of the potential energy barriers. To see this, consider motion in the one-dimensional potential $U_x(x) = \frac{Q}{2}[1 - \cos(2\pi x/L)]$, for which $D_{\text{eff}} = D_{\text{free}}/[I_0(\beta Q/2)]^2$, where I_0 is the zeroth-order modified Bessel function of the first kind. This is a monotonically decreasing function of the barrier height βQ, a fact reflected by the gradient $\partial D_{\text{eff}}/\partial(\beta Q)$, which is zero when $\beta Q = 0$ and negative for $\beta Q > 0$. As expected, adding—or increasing the size of—energy barriers reduces the effective diffusion coefficient. Although discussed here for a specific potential, this behavior is common to motion in one-dimensional periodic potentials: $\partial D_{\text{eff}}/\partial(\beta Q)$ is generally negative and at most vanishing at $\beta Q = 0$ [33,34]. Our quasi-one-dimensional system displays a more complicated behavior,

$$\left.\frac{\partial D_{\text{eff}}}{\partial \beta Q}\right|_{\beta Q=0} = -\frac{D_0\, \mathcal{C}(\alpha_0, \alpha_1)}{2}\cos\phi, \tag{14}$$

where $D_0 = D_{\text{eff}}(\beta Q = 0)$ and $\mathcal{C}(\alpha_0, \alpha_1)$ is a positive constant given by

$$\mathcal{C}(\alpha_0, \alpha_1) = \frac{\int_0^{2\pi} d\theta \cos\theta \sqrt{\alpha_0 + \alpha_1\cos\theta}}{\int_0^{2\pi} d\theta\, \sqrt{\alpha_0 + \alpha_1\cos\theta}} - \frac{\int_0^{2\pi} d\theta \cos\theta / \sqrt{\alpha_0 + \alpha_1\cos\theta}}{\int_0^{2\pi} d\theta\, / \sqrt{\alpha_0 + \alpha_1\cos\theta}}. \tag{15}$$

By varying the phase between the energy barriers and the curvature, it is possible for the gradient in Eq. (14) to become positive, indicating a behavior which cannot be observed in purely one-dimensional systems. This is the central result of our paper: adding energy barriers can enhance the rate of diffusion along the rugged channel.

In the following section, we compare our theoretical predictions—as given by Eq. (13)—with the results of numerical simulations. While agreement is expected when instantaneous equilibrium in the transverse direction can safely be assumed, our results allow us to assess the behavior of the system when this condition is not satisfied (e.g., when diffusion in the transverse direction proceeds at a finite rate). Remarkably, the counterintuitive enhancement of the diffusion coefficient with increasing barrier height survives up to equal transverse and longitudinal rates, thereby, demonstrating its experimental relevance and potential practical application.

IV. BROWNIAN DYNAMICS SIMULATIONS

We used Brownian dynamics simulations based on the overdamped Langevin equation to study the two main aspects of this paper: the effect of the phase difference ϕ upon the behavior of the effective diffusion coefficient and the cancellation of energetic and entropic barriers to motion when motion in the transverse direction is taken into account (and equilibration cannot be taken for granted). For the general form of the potential described in Eq. (1), the two-dimensional overdamped Langevin equation decomposes as follows:

$$\gamma_x \frac{dx}{dt} = -\frac{\partial U_x(x)}{\partial x} - \frac{\partial U_y(x,y)}{\partial x} + \xi_x(t),$$
$$\gamma_y \frac{dy}{dt} = -\frac{\partial U_y(x,y)}{\partial y} + \xi_y(t), \quad (16)$$

where $\xi(t)$ represents the thermal noise, which obeys the usual fluctuation-dissipation relationship $\langle \xi_{x,y}(t)\xi_{x,y}(t')\rangle = 2k_BT\gamma_{x,y}\delta(t-t')\delta_{x,y}$. Unless stated otherwise, simulations were performed with 10^5 noninteracting point particles, a time step $\delta t = 10^{-4}$ units, and unit values of the thermal energy k_BT and damping coefficients γ_x and γ_y. At each time step the particles' positions were advanced using the usual first-order Euler scheme [35]. Motion was simulated until the long-time diffusive regime was well established, and the effective diffusion coefficient was then extracted according to $D_{\text{eff}} = \lim_{t\to\infty}\langle x^2(t)\rangle/2t$. This regime is entered into once a substantial fraction of the ensemble of particles has explored beyond the first repeat unit of the potential energy landscape. By simulating for long enough that the root mean-squared displacement is equivalent to many repeat units, we can be confident that the dynamics have reached the long-time limit.

Equation (14) predicts that the gradient of the effective diffusion coefficient at $\beta Q = 0$ is proportional to $\cos\phi$. We performed simulations for $\phi = 0$ and $\phi = \pi$ to investigate the extremal cases. We will start with the former, because the behavior is familiar.

We expect a negative gradient at $\beta Q = 0$ and, hence, a monotonically decreasing effective diffusion coefficient. Figure 2 confirms these expectations and reveals good agreement between theory and simulations over a range of amplitudes. This is because the potential energy minima—around which the particles spend the bulk of their time—coincide with the points of minimum curvature. The distribution can get closer to its equilibrium shape in the regions of the channel where it would otherwise struggle most to do so. Agreement improves with increasing amplitude because more time is spent around the minima. Finally, agreement is better for smaller values of α_1 because the variations in curvature are smaller.

Let us now turn to the case of $\phi = \pi$. Equation (14) predicts that the effective diffusion coefficient initially grows with the amplitude of the potential energy barriers. Figure 3 confirms this and reveals qualitative agreement between theory and simulations. However, quantitative agreement is not as good as in the previous case. This is because the points of minimum curvature coincide with the potential energy maxima. These are unstable points, and particles pass through them quickly, leaving little chance for the ensemble to equilibrate. When $\alpha_1 = 1$ we see good quantitative agreement with the theory for values of $\beta Q > 2$. In contrast, for $\alpha_1 = 1.8$ there is a lack of good agreement even for $\beta Q = 4$. This is because the size of the entropic barriers to motion increases with the variation in the curvature of the channel, which is controlled by α_1. For smaller values of α_1, the rate of diffusion along the channel becomes determined by the height of the potential energy barriers at smaller values of the barrier height. Once in this regime, equilibration is less important for close

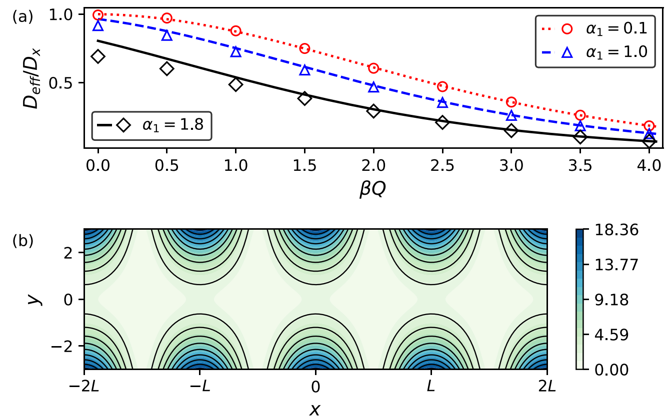

FIG. 2. Diffusion along the channel described by Eq. (8) is studied for the case of $\phi = 0$ where the potential minima coincide with the points of minimum curvature. (a) The diffusion coefficient D_{eff} is plotted as a function of the cosine barrier height for three values of α_1 where $\alpha_0 = 2$. A monotonic decrease is observed, and agreement between the simulation results (symbols) and the theory (lines) given in Eq. (13) improves with increasing barrier height. (b) A contour plot of the potential $U(x, y)$ used in the simulations. $\alpha_0 = 2$, $\alpha_1 = 1.8$, and $\beta Q = 1.25525$. Contours of constant potential (black lines) are drawn at regular intervals to guide the eye.

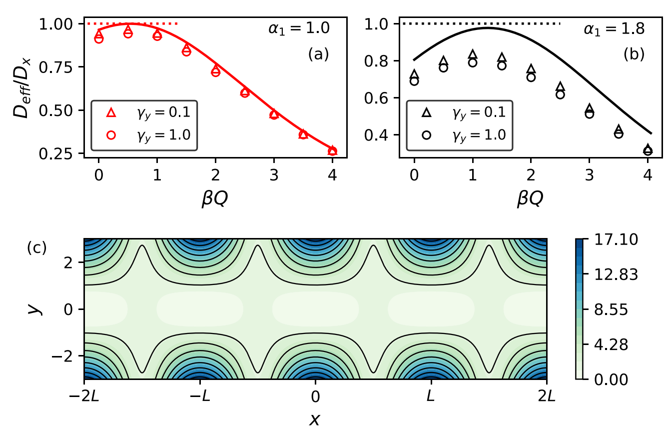

FIG. 3. Diffusion along the channel described by Eq. (8) is studied for the case of $\phi = \pi$ where the potential minima coincide with the points of maximum curvature. (a) and (b) The diffusion coefficient D_{eff} is plotted as a function of the cosine barrier height for two values of the damping coefficient in the y direction γ_y. D_{eff} initially increases with the height of the energy barriers, in contrast to Fig. 2 where a monotonic decrease is observed. Agreement between simulation results (symbols) and the theory (lines) given in Eq. (13) is better in (a), where $\alpha_1 = 1$, than (b), where $\alpha_1 = 1.8$. (c) A contour plot of the potential $U(x, y)$ used in the simulations. $\alpha_0 = 2$, $\alpha_1 = 1.8$, and $\beta Q = 1.25525$. Contours of constant potential (black lines) are drawn at regular intervals to guide the eye.

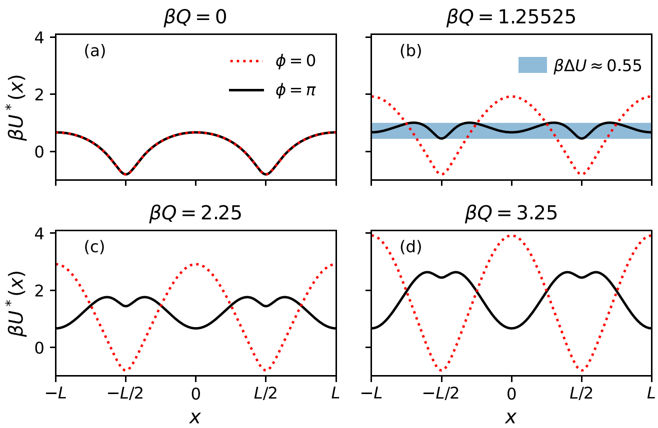

FIG. 4. The effective potential U^* given in Eq. (7) is plotted for the landscape described in Eq. (8). $\alpha_1 = 1.8$, $\alpha_0 = 2$. The panels (a)–(d) reveal how the effect of increasing the barrier height βQ on U^* depends strongly upon the phase difference ϕ between the barriers and the curvature. The contrasting behaviors—a monotonic increase in the amplitude of the potential ($\phi = 0$) vs a decrease followed by an increase ($\phi = \pi$)—the different response of the diffusion coefficient to increasing βQ observed in Figs. 2 and 3.

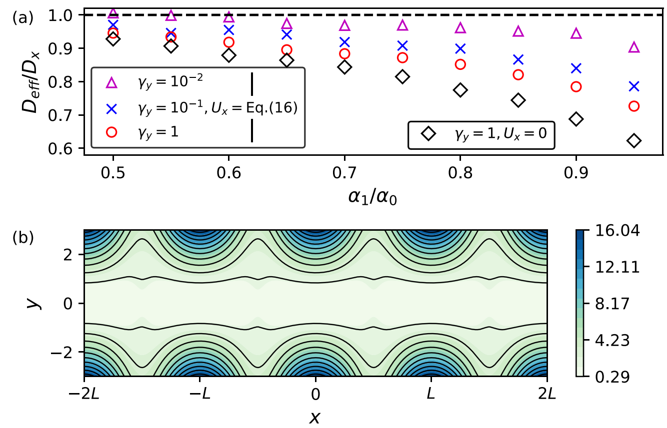

FIG. 5. Diffusion along the channel described by Eq. (17) is studied for the curvature profile $\alpha(x)$ given in Eq. (8). (a) The diffusion coefficient D_{eff} is plotted as a function of α_1/α_0 for a series of values of the damping coefficient in the y-direction γ_y ($\alpha_0 = 2$ throughout). Smaller values of γ_y give better agreement with the theoretical prediction (free diffusion) as expected for a theory based on the assumption of equilibration in the y direction. The effective diffusion coefficient in the absence of energy barriers ($U_x = 0$) is also plotted and observed to be smaller than in the presence of energy barriers: the barriers enhance the rate of diffusion. (b) The contour plot of $U(x, y)$ ($\alpha_0 = 2, \alpha_1 = 1.5$) reveals that the channel has a near-flat central section along x. Contours of constant potential (black lines) are drawn at regular intervals to guide the eye.

agreement with the theory. As expected, decreasing γ_y improves agreement with the theory.

Figure 4 provides insight into the origin of the behavior of the effective diffusion coefficient: Increasing the amplitude of the cosine potential does not necessarily increase the barrier to motion in the effective potential. The energetic and entropic contributions can interact with one another so as to *decrease* the barrier to motion as can be seen by comparing the panels for $\beta Q = 0$ and $\beta Q = 1.255\,25$, chosen because it is a good approximation to the amplitude which minimizes the barrier.

The contour plots in Figs. 2 and 3 illustrate this effect as well. Figure 2 reveals that introducing the cosine potential creates near-flat regions which extend away from the center of the channel. By contrast, the near-flat regions in Fig. 3 extend much further along the line of the channel than away from it. The former will inhibit motion along the channel by enabling particles to move significant distances in unproductive directions. The latter comes close to providing a continuous near-flat region along the line of the channel, which is combined with steeper barriers to motion away from it. The region either side of the center line is flatter in Fig. 3 than in Fig. 2, and the saddle points are broader, which is beneficial for transport; it is easier for particles to move from a tighter minimum into a broader saddle than vice versa.

Let us conclude this section by returning to a point made after the introduction of the effective potential in Eq. (7). The potential energy landscape,

$$U(x, y) = U_x(x) + U_y(x, y) = -\frac{1}{2\beta}\ln\left(\frac{\beta\alpha(x)}{2\pi}\right) + \frac{1}{2}\alpha(x)y^2 \quad (17)$$

has been constructed by adding to the U_y term describing the profile of the channel a series of potential energy barriers in the x direction U_x such that the effective potential U^* is exactly zero. This predicts free diffusion.

Motion was simulated for a range of values of α_1 for $\alpha_0 = 2$. In each case, the effect of decreasing γ_y from 10^0 to 10^{-2} upon the effective diffusion coefficient was studied. Motion was also simulated in the absence of the energy barriers. The results are shown in Fig. 5.

For all values of α_1 the effective diffusion coefficient is larger in the presence of energy barriers than in their absence. Again, as expected, decreasing γ_y improves agreement with the theory.

V. CONNECTION TO THE HARD-WALLED POTENTIAL

In this paper we chose to restrict our focus to soft-walled channels where the confining potential in the y direction permits particles to explore out to $y = \pm\infty$. The hard-walled potential, which features more commonly in the literature, can be viewed as a limiting form of the soft-walled case we studied.

Let us begin by considering Eq. (7), the expression for the effective potential $U^*(x)$,

$$U^*(x) = U_x(x) - \frac{1}{\beta}\ln\left(\int_{-\infty}^{\infty} dy\, e^{-\beta U_y(x,y)}\right). \quad (18)$$

The limits on the integral reflect the fact that the soft-walled potential is defined out to $y = \pm\infty$. However, if we consider a hard-walled potential which is flat between $y = \pm w(x)/2$ and infinite otherwise, then the expression for the effective potential becomes

$$\begin{aligned} U^*(x) &= U_x(x) - \frac{1}{\beta}\ln\left(\int_{-w(x)/2}^{w(x)/2} dy\right), \\ &= U_x(x) - \frac{1}{\beta}\ln[w(x)]. \end{aligned} \quad (19)$$

Having derived the hard-wall expression for the effective potential, let us draw the link between the soft- and hard-walled potentials. We chose to work with the potential described by

$$U_y(x, y) = \tfrac{1}{2}\alpha(x)y^2. \tag{20}$$

Suppose that we modify this expression to

$$U_y(x, y) = \tfrac{1}{2}[\alpha(x)y^2]^m, \tag{21}$$

where m is a positive integer and then rearrange it into the following form:

$$U_y(x, y) = \frac{1}{2}\left[\left(\frac{y}{w(x)/2}\right)^2\right]^m, \tag{22}$$

where we have defined $w/2 = \alpha^{-1/2}$.

Inserting Eq. (22) into the integral in Eq. (18) we find

$$\begin{aligned}\int_{-\infty}^{\infty} dy\, e^{-\beta U_y} &= \int_{-\infty}^{\infty} dy\, \exp\left[-\frac{\beta}{2}\left(\frac{y}{w/2}\right)^{2m}\right],\\ &= \frac{w}{2}\int_{-\infty}^{\infty} dz\, e^{-\beta z^{2m}/2},\end{aligned} \tag{23}$$

where, in moving from the first line to the second, we have changed variables to $y = z/(w/2)$. It can be demonstrated that the limiting value of the integral in Eq. (V) as $m \to \infty$ is two. Using this in Eq. (18), one obtains the same effective potential as in Eq. (19).

By drawing an explicit link between hard- and soft-walled potentials, we wish to point out that our results derived for the case of a soft-walled potential have, in fact, much broader relevance.

VI. CONCLUSIONS

We used the Fick-Jacobs equation to study the behavior of particles diffusing in soft-walled channels of periodically varying profile with potential energy barriers along their length. Treating the variations in the profile of the channel as entropic barriers to motion reduces the problem to diffusion in an (approximate) one-dimensional potential.

For the cosine-based potential studied here, the position of the potential energy minima relative to the points of minimum curvature determines how the effective diffusion coefficient responds to increasing the height of the energy barriers. If the two coincide, then a monotonic decrease is observed, and there is good quantitative agreement between numerical simulations and theory. If the two are perfectly out of phase so that the energy minima coincide with the regions of maximum curvature, then the effective diffusion coefficient initially increases above its zero-amplitude value, resulting in enhanced diffusion. Good quantitative agreement is observed only when the energy barriers dwarf the entropic barriers. Before this point, lack of equilibration in the confining direction precludes good agreement.

For a given channel it is possible to construct a series of energy barriers which cancel out the entropic barriers; free diffusion is then predicted. Numerical simulations confirm that adding these barriers increases the rate of diffusion, and decreasing the damping coefficient in the confining direction leads ever closer to free diffusion.

Further work could explore the behavior of the system when the curvature varies as a function of time [36,37]. Likewise, studying the motion of active particles might produce some interesting results [38,39].

ACKNOWLEDGMENTS

This work was supported, in part, by the Nanyang Technological University, Singapore under its Start Up Grant Scheme No. 04INS000175C230 (E.H.Y.) and by the Engineering and Physical Sciences Research Council (EPSRC) Grant No. EP/P034616/1 (C.C. and T.H.G.).

[1] D. M. Ruthven, Diffusion in zeolites, in *Zeolites: A Refined Tool for Designing Catalytic Sites*, edited by L. Bonneviot and S. Kaliaguine, Studies in Surface Science and Catalysis Vol. 97 (Elsevier, Amsterdam, 1995), pp. 223–234.

[2] A. Schüring, S. M. Auerbach, S. Fritzsche, and R. Haberlandt, On entropic barriers for diffusion in zeolites: A molecular dynamics study, J. Chem. Phys. **116**, 10890 (2002).

[3] D. Reguera, G. Schmid, P. S. Burada, J. M. Rubi, P. Reimann, and P. Hanggi, Entropic Transport: Kinetics, Scaling, and Control Mechanisms, Phys. Rev. Lett. **96**, 130603 (2006).

[4] B. Hille, Ionic channels in excitable membranes. Current problems and biophysical approaches, Biophys. J. **22**, 283 (1978).

[5] A. M. Berezhkovskii and S. M. Bezrukov, Optimizing transport of metabolites through large channels: Molecular sieves with and without binding, Biophys. J. **88**, L17 (2005).

[6] L. Liu, P. Li, and S. A. Asher, Entropic trapping of macromolecules by mesoscopic periodic voids in a polymer hydrogel, Nature (London) **397**, 141 (1999).

[7] A. Corma, From microporous to mesoporous molecular sieve materials and their use in catalysis, Chem. Rev. **97**, 2373 (1997).

[8] D. Reguera, A. Luque, P. S. Burada, G. Schmid, J. M. Rubi, and P. Hanggi, Entropic Splitter for Particle Separation, Phys. Rev. Lett. **108**, 020604 (2012).

[9] T. Motz, G. Schmid, P. Hanggi, D. Reguera, and J. M. Rubi, Optimizing the performance of the entropic splitter for particle separation, J. Chem. Phys. **141**, 074104 (2014).

[10] A. Berezhkovskii and G. Hummer, Single-File Transport of Water Molecules through a Carbon Nanotube, Phys. Rev. Lett. **89**, 064503 (2002).

[11] P. S. Burada, P. Hänggi, F. Marchesoni, G. Schmid, and P. Talkner, Diffusion in confined geometries, ChemPhysChem **10**, 45 (2009).

[12] M. H. Jacobs, Diffusion processes, in *Diffusion Processes* (Springer, Berlin/Heidelberg, 1935), pp. 1–145.

[13] A. Fick, Ueber diffusion, Ann. Phys (NY) **170**, 59 (1855).

[14] R. Zwanzig, Diffusion past an entropy barrier, J. Phys. Chem. **96**, 3926 (1992).

[15] D. Reguera and J. M. Rubi, Kinetic equations for diffusion in the presence of entropic barriers, Phys. Rev. E **64**, 061106 (2001).

[16] T. H. Gray and E. H. Yong, An effective one-dimensional approach to calculating mean first passage time in multi-dimensional potentials, J. Chem. Phys. **154**, 084103 (2021).

[17] P. Kalinay and J. K. Percus, Projection of two-dimensional diffusion in a narrow channel onto the longitudinal dimension, J. Chem. Phys. **122**, 204701 (2005).

[18] P. Kalinay and J. K. Percus, Corrections to the fick-jacobs equation, Phys. Rev. E **74**, 041203 (2006).

[19] P. Kalinay and J. K. Percus, Approximations of the generalized fick-jacobs equation, Phys. Rev. E **78**, 021103 (2008).

[20] P. Burada, G. Schmid, P. Talkner, P. Hanggi, D. Reguera, and J. Rubi, Entropic particle transport in periodic channels, Biosystems **93**, 16 (2008).

[21] P. S. Burada, G. Schmid, D. Reguera, J. M. Rubi, and P. Hanggi, Biased diffusion in confined media: Test of the fick-jacobs approximation and validity criteria, Phys. Rev. E **75**, 051111 (2007).

[22] P. Burada, Y. Li, W. Riefler, and G. Schmid, Entropic transport in energetic potentials, stochastic processes in Physics and Chemistry (in honor of P. Hanggi), Chem. Phys. **375**, 514 (2010).

[23] X.-T. Zheng, J.-C. Wu, B.-Q. Ai, and F.-G. Li, Brownian pump induced by the phase difference between the potential and the entropic barrier, Eur. Phys. J. B **86**, 479 (2013).

[24] R. M. Bradley, Diffusion in a two-dimensional channel with curved midline and varying width: Reduction to an effective one-dimensional description, Phys. Rev. E **80**, 061142 (2009).

[25] A. Berezhkovskii and A. Szabo, Time scale separation leads to position-dependent diffusion along a slow coordinate, J. Chem. Phys. **135**, 074108 (2011).

[26] L. Dagdug and I. Pineda, Projection of two-dimensional diffusion in a curved midline and narrow varying width channel onto the longitudinal dimension, J. Chem. Phys. **137**, 024107 (2012).

[27] Y. Chavez, G. Chacon-Acosta, and L. Dagdug, Effects of curved midline and varying width on the description of the effective diffusivity of brownian particles, J. Phys.: Condens. Matter **30**, 194001 (2018).

[28] X. Wang and G. Drazer, Transport of brownian particles in a narrow, slowly varying serpentine channel, J. Chem. Phys. **142**, 154114 (2015).

[29] X. Wang, Biased transport of brownian particles in a weakly corrugated serpentine channel, J. Chem. Phys. **144**, 044101 (2016).

[30] F.-g. Li and B.-q. Ai, Current control in a two-dimensional channel with nonstraight midline and varying width, Phys. Rev. E **87**, 062128 (2013).

[31] J. Alvarez-Ramirez, L. Dagdug, and L. Inzunza, Asymmetric brownian transport in a family of corrugated two-dimensional channels, Physica A **410**, 319 (2014).

[32] C. Gardiner, *Handbook of Stochastic Methods for Physics, Chemistry, and the Natural Sciences*, Springer Complexity (Springer, Berlin, Heidelberg, 2004).

[33] S. Lifson and J. L. Jackson, On the self-diffusion of ions in a polyelectrolyte solution, J. Chem. Phys. **36**, 2410 (1962).

[34] R. Zwanzig, Diffusion in a rough potential, Proc. Natl. Acad. Sci. USA **85**, 2029 (1988).

[35] D. L. Ermak and J. A. McCammon, Brownian dynamics with hydrodynamic interactions, J. Chem. Phys. **69**, 1352 (1978).

[36] S. Marbach, D. Dean, and L. Bocquet, Transport and dispersion across wiggling nanopores, Nat. Phys. **14**, 1108 (2018).

[37] Y. Li, F. Marchesoni, D. Debnath, and P. K. Ghosh, Non-gaussian normal diffusion in a fluctuating corrugated channel, Phys. Rev. Research **1**, 033003 (2019).

[38] F.-g. Li, H.-z. Xie, X.-m. Liu, and B.-q. Ai, The influence of a phase shift between the top and bottom walls on the brownian transport of self-propelled particles, Chaos **25**, 033110 (2015).

[39] F.-G. Li and B.-Q. Ai, Manipulating channel asymmetries to control the mobility and diffusion of anisotropic particles, Physica A **484**, 27 (2017).